Energy Harvesting from Bicycle Vibrations

Alberto Doria, Edoardo Marconi, Federico Moro, *Member IEEE*

Dipartimento di Ingegneria Industriale
Università degli Studi di Padova
Via Venezia 1, 35131 Padova, Italy
alberto.doria@unipd.it, edoardo.marconi@unipd.it, federico.moro@unipd.it

***Abstract*—The problem of frequency tuning a cantilever piezo-harvester to the typical vibrations of a bicycle is here investigated. This is key to optimize the energy harvesting performance. Road tests with a bicycle on a typical city track are first carried out to measure the power spectral density of bike vibrations. Both analytical and experimental methods are used to estimate the average electric power that can be harvested by a piezo-harvester with a solid tip mass. This solution is compared to a tuning strategy based on a liquid tip mass by using a novel analytical method for simulating frequency response.**

***Index Terms*—Bicycle, harvester, tuning, energy harvesting, piezoelectric, liquid mass, stress, vibrations, low-emission mobility.**

I. Introduction

In recent years there has been a great development of energy harvesting technologies for powering small devices such as portable electronics, sensors, and transmitters without the need for battery replacement or complex wiring systems [1][2]. Vibration energy harvesting (VEH) represents a viable solution for harvesting small amounts of electric power from kinetic energy of environmental vibrations [3]. Energy harvesting from vortex vibrations induced in a fluid flow was investigated in [4]. Piezo-harvesters for harvesting energy from raindrops [5] and body motion [6] were also proposed in literature.

Bicycles have nowadays become very popular for everyday use and are key to target low-emission mobility policies set by most governments to face climate changes. The rolling motion of wheels on a road generates significant vibrations in many parts of a bike, which are suitable for harvesting. Plane rotary electromagnetic generators were proposed in [7] to replace conventional dynamos, whereas a harvester based on rotating magnets and induction coils was developed in [8]. Both devices were able to power LED lights. A wireless speed sensor that collects energy from wheel rotation and senses the wheel speed was presented in [9]. An electromagnetic harvester able to collect energy from the weaving motion of a bike was presented in [10]. The possibility of harvesting from bike vibrations with piezo-harvesters was studied by Minazara [11]. Experimental tests carried out by the same authors showed that the harvested power (around 9 mW for an acceleration of 8 m/s^2) was enough to power a small on-board calculator or a flash lighting of the bike [12]. A prototype of a piezoelectric harvesting system for bikes, capable of outputting 13.6 mW electric power at regular cycling speed, has been recently proposed in [13].

This work investigates the problem of tuning a low-cost cantilever piezo-harvester to the typical vibrations of a bicycle running on a city track. The analysis of some preliminary experimental results in [14] has shown that most of the kinetic energy associated to bike vibrations is concentrated in a narrow frequency band below 30 Hz. Since cantilever piezo-harvesters attain their best performance much beyond this limit, specific tuning strategies have to be adopted. The possibility of using auxiliary oscillators for tuning cantilever piezo-harvesters was investigated in [15]. It was shown that an auxiliary oscillator with a small mass (5 g) has almost the same effect of a larger tip mass (17 g) in terms of output voltage and stress inside the piezo-layer. Starting from first experimental evidence presented in [14], in this work a liquid tip mass is used for further reducing stress inside materials compared to the solid tip mass solution, often used in the engineering practice. The tuning solution based on a liquid mass is eco-friendly and can be marketed without any problem, differently from solid mass tuning which makes use of lead. Conversely, volumetric power density of the harvester with liquid tip mass is lower than the one of the harvester with solid tip mass. A novel mathematical model of the water sloshing in the tip container, which allows the prediction of the frequency response function (FRF) of a harvester with liquid tip mass, is presented and experimentally validated.

This paper is organized as follows. Section II is concerned with experimental measurements of bike vibrations on a typical city track. Starting from these measurements, the output voltage frequency behavior of a cantilever piezo-harvester with solid tip mass is predicted in Section III. A novel analytical model for simulating the FRF of a piezo-harvester with liquid mass in horizontal and vertical configurations is presented in Section IV. According to simulation results, harvesters tuned to bike vibrations are developed and tested in order to measure their response in Section V. Section VI deals with the prediction of harvested electric power for all considered harvester set-ups. Section VII shows the effect on liquid mass on stress. Finally, conclusions are drawn.

II. Bicycle Vibrations

In the framework of this research a typical step-through city bike was tested on a city track, in order to characterize the

sources of vibrations that could be exploited by the harvesters. The test speed was constant (15 km/h). Fig. 1 shows the testing equipment mounted on the bicycle. The accelerations of the steerer tube and of the seatpost (under the saddle) were measured by means of a triaxial accelerometer (Midé SlamStick LOG-0003-16G-8GB-PC). These two locations are selected because (i) they are easily accessible and (ii) the harvester mounted in these positions would not interfere with the rider. Additional locations, where a high level of vibrations is present, may be identified by a dedicated analysis; however, this investigation is out of the scope of this work, which is focused on harvester tuning strategies. Fig. 2 shows typical time records of the measured accelerations of the steerer tube of the step-through frame bike in the longitudinal (a_x), lateral (a_y), and vertical directions (a_z). The power spectral densities (PSDs) of the measured accelerations were calculated by means of a MATLAB® code. Fig. 3 shows the PSDs of the components of steerer tube and seatpost acceleration. The largest acceleration levels appear on the steerer tube. In both points the acceleration components with largest intensity are a_x and a_z.

Fig. 1. Accelerometer mounted on the steerer tube.

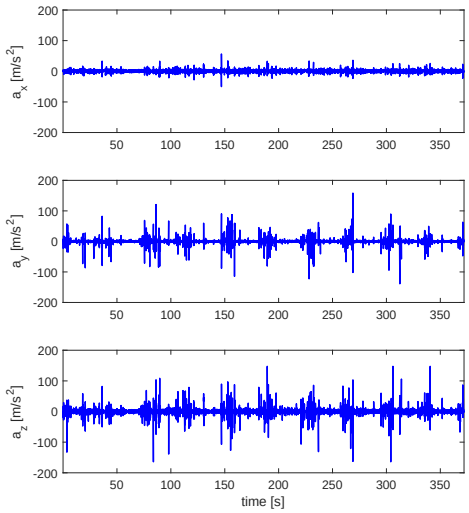

Fig. 2. Measured acceleration of the steerer tube at 15 km/h.

Acceleration PSDs give useful information about the distribution of vibration energy in the frequency domain. Most of the vibration energy is concentrated in the range from 0 to 40 Hz. This typical phenomenon happens because in bicycles the high-frequency excitation from the road is filtered by the tire enveloping effect [16]. Therefore, many high-frequency modes of vibration of the bicycle, that are related to the structural deformation of frame and forks, are not significantly excited.

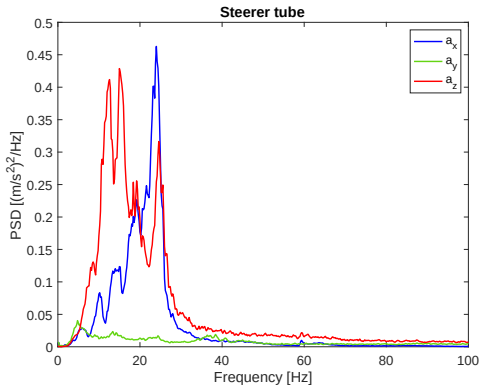

(a)

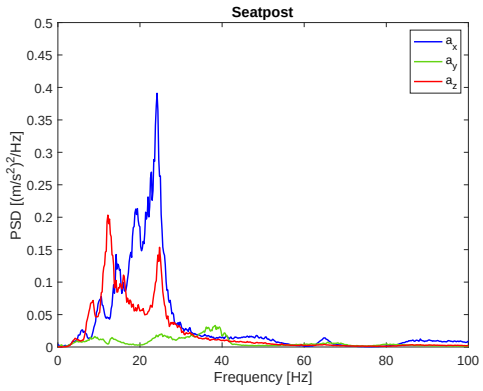

(b)

Fig. 3. Acceleration PSDs of the steerer tube (a) and seatpost (b).

The peaks that appear in the PSDs of Fig. 3 are mainly related to the excitation of the low-frequency structural modes, and of the rigid-body modes of the bicycle, in which the bike with the rider essentially behaves as a rigid body mounted on elastic springs that represent the effect of tire deformability. Fig. 4 shows the relevant modes of vibration of the tested bicycle. The modal shapes were obtained in ABSignal ModalVIEW by performing an experimental modal analysis of the bike [17], which also included the rider. The structure of the vehicle was discretized with a 15-node mesh. The modes at 12.53 Hz and 16.87 Hz are rigid body modes – named bounce and pitch, respectively – dominated by tire deformability: note how the structural parts of the bike (fork and frame) do not undergo relevant deformations in these modes. The mode at 27.2 Hz is the first structural mode, which shows relevant in-opposition displacements of the handlebar and the seatpost, and is responsible for the highest PSD peaks in the longitudinal direction.

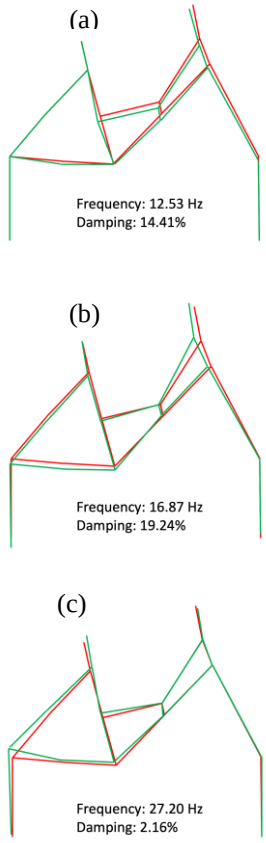

Fig. 4. Modes of vibration of the bicycle: (a) first mode, (b) second mode, and (c) third mode (red: undeformed mesh, green: deformed mesh).

III. Vibration Energy Harvesting by Means of Piezoelectric Cantilevers with Solid Tip Mass

A piezoelectric unimorph harvester (Midé PPA-1001) in cantilever configuration was considered. The harvested power can be estimated with good accuracy from experimental acceleration data once the FRF of the energy harvester has been properly predicted by an analytical model.

This energy harvester consists of a single piezoceramic layer, which converts strain into electrical voltage, and a structural layer (stainless steel). The harvester excitation is provided by the base acceleration at the clamped end, whereas the other end is bonded to a tip mass for the resonance frequency tuning. The frequency response of the harvester is analytically computed by a single-mode electromechanical distributed-parameter model, such as the one derived by Inman and Erturk [18].

The frequency response function between the open-circuit voltage and the base acceleration is useful to assess the optimal frequency band for exploiting the harvester and to tune it to the vibration source. This FRF can also be employed to design advanced circuits for energy conversion. As already noted in Section II, typical vibration sources related to bike motion are in a low-frequency range, much lower than the natural frequency of the harvester. The addition of a tip mass M_t is the simplest method that can be used for tuning the harvester to the vibration source. For a unimorph cantilever piezo-harvester, excited at angular frequency ω close to the angular frequency ω_1 of the first mode, the open-circuit FRF is [18]:

$$FRF_{\mathrm{OC}}(\omega) = \frac{-\varphi_1^u \left[\int_0^L \mu\, \phi_1(x)\, dx + M_t\, \phi_1(L)\right]}{C_{pu}(\omega_1^2 - \omega^2 + 2i\,\zeta_1\omega_1\omega) + \varphi_1^u \chi_1^u} \qquad (1)$$

where C_{pu} is the capacitance of the piezoelectric layer, μ is the mass per unit length, and the parameters evaluated at the first mode are: the forward and the backward modal coupling coefficients φ_1^u and χ_1^u, the vibration mode ϕ_1, and the damping ratio ζ_1.

The open-circuit FRF makes it possible to obtain the PSD of the open-circuit voltage in the frequency domain $S_{V_{OC}}(\omega)$ from the PSD of the measured base acceleration $S_A(\omega)$, as:

$$S_{V_{OC}}(\omega) = |FRF_{\mathrm{OC}}(\omega)|^2\, S_A(\omega) \qquad (2)$$

Fig. 3 highlights that a piezo-harvester can collect a relevant amount of energy from bike vibrations only if it is tuned to a frequency lower than 40 Hz, whereas the standard PPA 1001 harvester considered in this research has a resonance frequency of 120 Hz. Therefore, a tuning strategy has to be adopted. Fig. 5 depicts the open-circuit FRFs of the PPA 1001 alone and with two tip masses predicted from (1). It can be noted that a 4 g tip mass is sufficient to move the resonance frequency from 120 Hz to 40 Hz. A rather large tip mass (17 g) is needed to lower the resonance frequency down to 20 Hz, i.e., within the frequency band of bike vibrations (0-40 Hz).

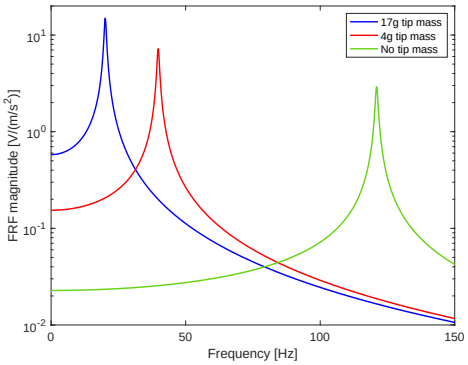

Fig. 5. Open-circuit FRF of the harvester with tip masses of various size.

Fig. 6 shows the open-circuit voltage PSDs obtained with (2) from the experimental acceleration PSDs in Fig. 3, measured on the steerer tube. The harvester with no tip mass is excited by very low vibration levels that are present in the acceleration PSD at 120 Hz. Consequently, the PSD of generated voltage is negligible. When a tuning frequency of 40 Hz is achieved, the harvester operates at the limit of the frequency band of bike vibrations and the output voltage increases compared to the case of the harvester with no tip mass. Finally, only the harvester tuned to 20 Hz is able to satisfactorily exploit bike vibrations.

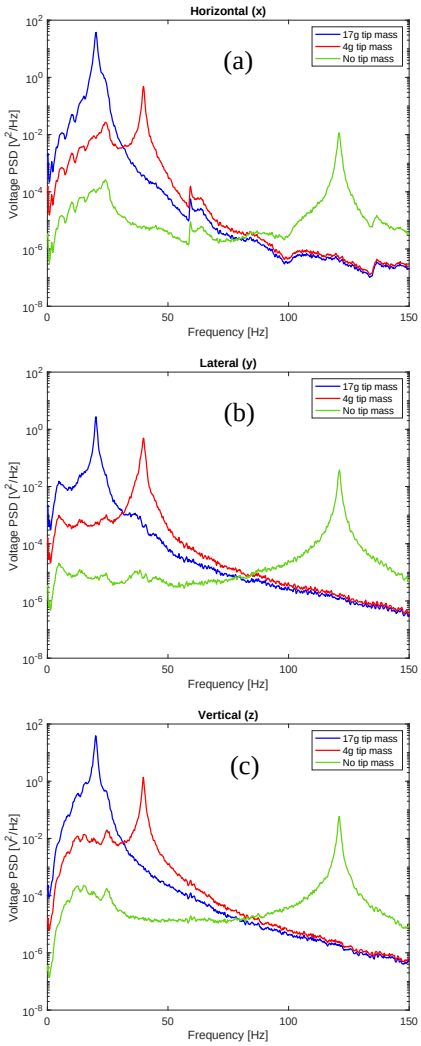

Fig. 6. Open-circuit voltage PSD at three tuning frequencies: horizontal (a), lateral (b), and vertical (c) excitation.

Fig. 6 confirms the need for a strong decrease in the natural frequency of the harvester and shows two limits of the tuning by means of a simple tip mass. Firstly, the operating bandwidth of the harvester is rather narrow. Secondly, the large increase in the generated voltage is beneficial, but it corresponds to a large increase in the stress inside the piezoelectric material. This effect can be explained considering the matrix equation of a piezoelectric material [18]:

$$\begin{pmatrix} T_1 \\ D_3 \end{pmatrix} = \begin{pmatrix} c_{11}^E & -e_{31} \\ e_{31} & \varepsilon_{33}^S \end{pmatrix} \begin{pmatrix} S_1 \\ E_3 \end{pmatrix} \quad (3)$$

which relates the mechanical stress T_1 (in longitudinal direction) and the electric displacement D_3 (in transverse direction) with the strain S_1 and electric field E_3 components in the same directions. Matrix coefficients in (3) are: the Young's modulus at constant electric field c_{11}^E, the piezoelectric constant e_{31}, and the permittivity at constant strain ε_{33}^S. From (3) it can be deduced that, when a solid tip mass is added, the increase in the output voltage in Fig. 6 – and in turn in D_3 – is due to an increase in S_1, which subsequently leads to an increase in T_1.

Many piezoelectric materials are ceramics with a limited fatigue strength [19][20][21]. This issue is crucial in applications, like bike energy harvesting, in which some tens of thousands of loading cycles are reached in only one hour of operation.

IV. Vibration Energy Harvesting by means of Piezoelectric Cantilvers with Liquid Tip Mass

The possibility of using liquid filled masses in order to broaden the bandwidth of the harvester was first studied in [22][23]. In this research the variation in time of the resonant frequency was calculated with the model presented in [24]. Further developments of the research on liquid-filled masses included the use of different liquids: glycerin, honey and motor oil in [25], liquid metal in [26]. In [27] the possibility of using a magnetic actuation to control the location of a ferro-fluid liquid was analyzed. Finally, in [28] the free motion of cylinders in a liquid was exploited to broaden the harvester bandwidth.

The key idea of this work is to use a liquid-filled mass to tune a harvester to low-frequency vibrations in order to improve harvesting performance, and at same time to reduce the stress level inside the piezoelectric material in comparison with the solid mass tuning. The mathematical model of the harvester with liquid tip mass is developed using sloshing motion dynamics, instead of using the movable mass theory [22][24]. The sloshing motion takes place when a container filled with liquid vibrates, and the liquid only partially follows the motion of the container, owing to the appearance of surface waves. This phenomenon has been studied in many fields of engineering for many years [29]-[31]. Nevertheless, up to now sloshing models have not been widely used to study harvesters with liquid tip mass. Only in [32] a non-linear sloshing model is introduced to interpret experimental results. Even though an accurate simulation of sloshing motions would require a non-linear model with a large number of Degrees of Freedom (DOFs), an approximate but realistic representation of liquid dynamics inside the container can be obtained by means of a lumped-element approach. According to this representation, the liquid is divided into a portion m_0 that vibrates with the container and some portions m_i, $i = 1,..,N$, that are connected to the walls of the container by means of equivalent springs with stiffness k_i [29]. More masses make it possible to consider more sloshing modes in the model. This lumped-element approach is well suited for the multi-physic simulation of a cantilever harvester with liquid tip mass. Harvesters for vertical and horizontal vibrations are schematized according to the representations of Fig. 7 and Fig. 8. The first sloshing mode, which is the most important, is simulated considering only a single moving mass ($N = 1$). The parameters of the model, which also include the moment of inertia I_0 of the first mass and the positions of the masses with respect to the container base hb_0 and hb_1, are calculated with the approach proposed in [29]. The cantilever harvester is simulated as a cantilever beam with a vibrating base.

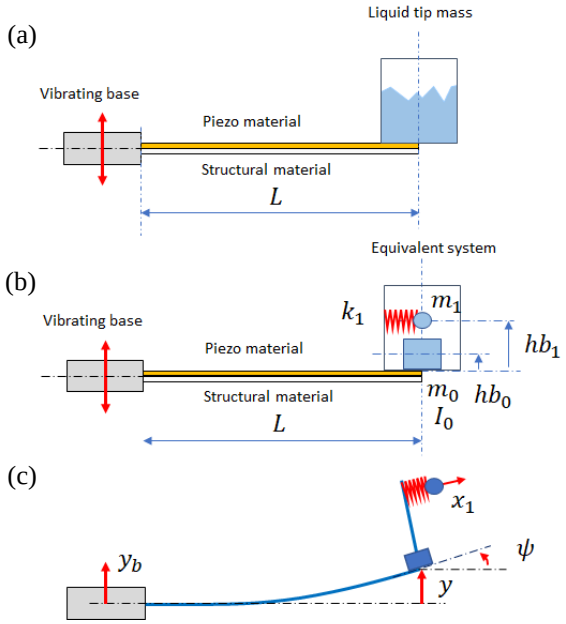

Fig. 7. (a) Harvester for vertical vibrations; (b) Equivalent spring-mass system to model sloshing; (c) Scheme of DOFs.

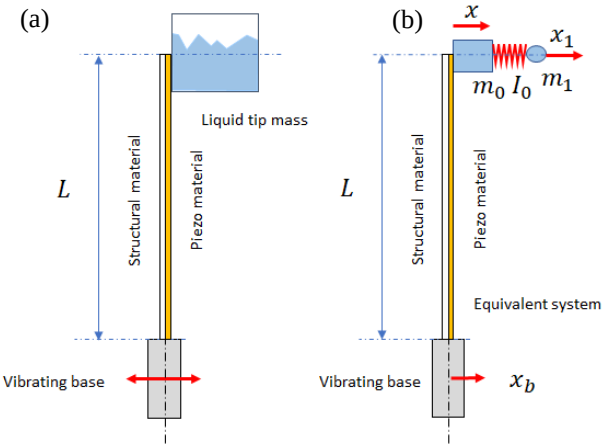

Fig. 8. (a) Harvester for horizontal vibrations; (b) Equivalent spring-mass system to model sloshing.

A. Lumped-element model for vertical base excitation

The equivalent dynamic model of a harvester for vertical vibrations has 3 DOFs (Fig. 7c): the vertical base displacement y_b, the cantilever tip rotation ψ (which is related to tip displacement y by beam theory equations), and the relative displacement x_1 of mass m_1 with respect to the container.

The cantilever beam is modeled according to a lumped-element approach by means of a lumped stiffness in the transverse direction k_y and a lumped mass m_s, given by:

$$k_y = 3\frac{EJ}{L^3} \tag{4}$$

$$m_s = \frac{33}{140}\mu L + m_c \tag{5}$$

where L is the beam length, E is the Young modulus, J is the moment of inertia of the composite cross section of the harvester, μ is the mass per unit length of the harvester, and m_c is the mass of the container.

The displacement of the beam tip is related to tip rotation by:

$$y = \frac{2}{3}\psi L \tag{6}$$

The equivalent stiffness along the ψ coordinate is:

$$k_\psi = k_y\left(\frac{2}{3}L\right)^2 \tag{7}$$

In order to account for the energy dissipation, equivalent viscous dampers c_ψ and c_1 in parallel with the elastic elements are considered [33].

By using the Lagrange method, the following equations of motion are obtained:

$$\begin{bmatrix} m_s\frac{4}{9}L^2 + I_0 + m_0\left(hb_0{}^2 + \frac{4}{9}L^2\right) + m_1\left(hb_1{}^2 + \frac{4}{9}L^2\right) & -hb_1m_1 \\ -hb_1m_1 & m_1 \end{bmatrix}\begin{Bmatrix}\ddot{\psi}\\ \ddot{x}_1\end{Bmatrix} + \begin{bmatrix} c_\psi & 0 \\ 0 & c_1\end{bmatrix}\begin{Bmatrix}\dot{\psi}\\ \dot{x}_1\end{Bmatrix} + \begin{bmatrix} k_\psi - g(hb_0m_0 + hb_1m_1) & gm_1 \\ gm_1 & k_1\end{bmatrix}\begin{Bmatrix}\psi\\ x_1\end{Bmatrix} = \begin{Bmatrix}-\frac{2}{3}L(m_s + m_0 + m_1)\ddot{y}_b(t)\\ 0\end{Bmatrix} \tag{8}$$

By enforcing a harmonic base acceleration:

$$\ddot{y}_b(t) = a_{b0}sin(\omega t) \tag{9}$$

the FRFs of ψ and y with respect to the base acceleration a_{b0} are obtained from (8) and (6).

According to Erturk and Inman [34], the output voltage v of a cantilever piezo-harvester in unimorph configuration depends on the relative displacement transverse to the beam w_r, as:

$$C_{pu}\frac{dv(t)}{dt} + \frac{v(t)}{R} = -e_{31}bh_{pc}\int_0^L \frac{\partial^3 w_r(x,t)}{\partial x^2 \partial t}dx \tag{10}$$

where C_{pu} is the internal capacitance of the piezoelectric layer, R the resistance of the external load, e_{31} is the piezoelectric constant, b is the width of the piezoelectric layer, and h_{pc} is the distance between the neutral axis of the composite cross section and the center of the piezoelectric layer. In open-circuit condition, by letting $R \to \infty$ in (10), one obtains:

$$C_{pu}v(t) = -e_{31}bh_{pc}\int_0^L \frac{\partial^2 w_r(x,t)}{\partial x^2}dx \tag{11}$$

The transverse displacement along the beam axis can be approximated as a function of lumped-element parameter y:

$$w_r(x,t) \approx yg(x)\sin(\omega t) \tag{12}$$

where g is a function of the axial coordinate x. By letting (12) in (11), the open-circuit voltage in time domain becomes:

$$v(t) = -\frac{e_{31}bh_{pc}}{C_{pu}}y\sin(\omega_n t)\int_0^L \frac{\partial^2 g(x)}{\partial x^2}dx \tag{13}$$

whose amplitude is:

$$V_{OC,max} = -\frac{e_{31}bh_{pc}}{C_{pu}}\left(\frac{\partial g(L)}{\partial x} - \frac{\partial g(0)}{\partial x}\right)y \tag{14}$$

B. Lumped model for horizontal base excitation

The dynamic model used to study the response of the harvester with horizontal base excitation (Fig. 8b) is similar to the previous model. The equivalent parameters of water for the first sloshing mode are calculated considering the different shape and size of the container in the horizontal direction [35].

Fig. 8 shows that base excitation is associated to coordinate x_b, whereas the displacements of the cantilever tip and of the moving mass m_1 are associated to coordinates x and x_1 respectively. Coordinate x is related to tip rotation as for y in (6). The equations of motion are:

$$\begin{bmatrix} m_1+m_0+m_s+\frac{9}{4}\frac{I_0}{L^2} & m_1 \\ m_1 & m_1 \end{bmatrix}\begin{Bmatrix}\ddot{x}\\ \ddot{x}_1\end{Bmatrix} + \begin{bmatrix} c_x & 0 \\ 0 & c_1 \end{bmatrix}\begin{Bmatrix}\dot{x}\\ \dot{x}_1\end{Bmatrix} + \begin{bmatrix} k_x & 0 \\ 0 & k_1 \end{bmatrix}\begin{Bmatrix}x\\ x_1\end{Bmatrix} = \begin{Bmatrix}-(m_s+m_0+m_1)\ddot{x}_b(t)\\ -m_1\ddot{x}_b(t)\end{Bmatrix} \quad (15)$$

They are solved in the presence of harmonic base excitation and open-circuit voltage is calculated according to (14).

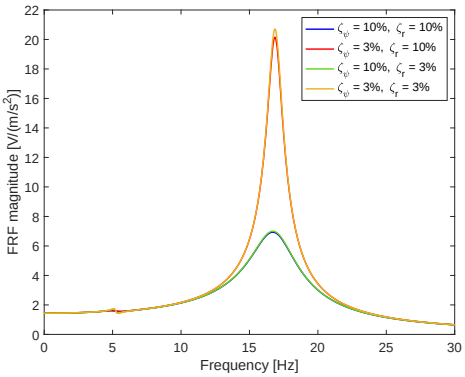

Fig. 9. Open-circuit FRF of the harvester with liquid tip mass, harvesting vertical vibrations (ζ_ψ, ζ_r are the harvester and sloshing damping ratios).

C. Open-circuit frequency response

The FRFs between open-circuit voltage and base acceleration of the harvester with liquid tip mass (17 g as the largest solid tip mass) are shown in Fig. 9 and Fig. 10 for the vertical and horizontal configurations, respectively. In both cases, parametric values of the damping ratio of the harvester [33] and of the equivalent spring-mass system that models sloshing are considered. The damping ratios are obtained assuming that DOFs are uncoupled:

$$\zeta_\psi = \frac{c_\psi}{2\sqrt{k_\psi\left(m_s\frac{4}{9}L^2+I_0+m_0\left(hb_0{}^2+\frac{4}{9}L^2\right)+m_1\left(hb_1{}^2+\frac{4}{9}L^2\right)\right)}} \quad (16)$$

$$\zeta_r = \frac{c_1}{2\sqrt{k_1 m_1}} \quad (17)$$

$$\zeta_x = \frac{c_x}{2\sqrt{k_x\left(m_1+m_0+m_s+\frac{9I_0}{4L^2}\right)}} \quad (18)$$

In the vertical configuration, with the parameters of the present prototype the resonance frequencies are f_1=5.12 Hz and f_2=16.63 Hz. The first resonance peak is very small because it corresponds to a mode of vibration that chiefly involves the liquid. The second resonance peak corresponds to a mode of vibration with a relevant cantilever bending that generates electrical voltage owing to the piezoelectric effect.

In the horizontal configuration, the resonance frequencies are f_1=4.42 Hz and f_2=22.62 Hz. In this case both resonances correspond to the excitation of modes of vibration with cantilever bending and generation of voltage.

In both configurations, since in (8) and (15) the off-diagonal terms couple the two displacements, it is not possible to adjust one resonance frequency independently from the other.

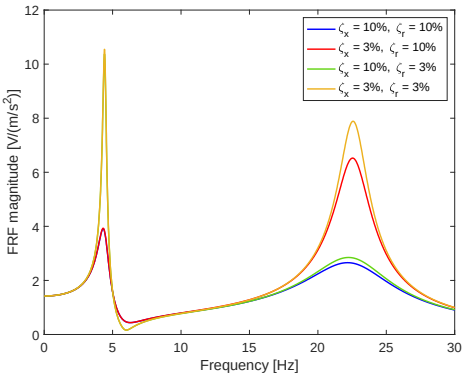

Fig. 10. Open-circuit FRF of the harvester with liquid tip mass, harvesting horizontal vibrations (ζ_x, ζ_r are the harvester and sloshing damping ratios).

It is worth noticing that liquid mass tuning makes it possible to have two slightly different tuning frequencies in the two directions and this phenomenon can be exploited if the excitation PSDs in the two directions are different.

V. Experimental Results

The response of the harvester with the solid and liquid tip masses was experimentally measured. The solid tip mass (lead) was 17 g, the liquid mass (water) including the container had the same value. The volume of the liquid mass with container was 27 cm^3 whereas the solid mass volume was 1.5 cm^3.

The piezo-harvester was attached to a permanent-magnet electrodynamic shaker through a custom-built clamp, and a sinusoidal acceleration of the base of the cantilever was imposed. The actual acceleration of the clamp and the voltage generated by the piezo-harvester were recorded by a module for sound and vibration measurements. The tests were carried out at various constant frequencies in the 5–100 Hz range, and the response of the harvester was quantified by the ratio between the voltage RMS and the base acceleration RMS. The harvester with solid tip mass was tested in the configuration in Fig. 11, with vertical shaker axis. In order to account for the different distribution of the liquid within the container, the harvester with the liquid tip mass was tested in the configurations in Fig. 12.

In the next section, the measured harvester response is used, in conjunction with the PSD of accelerations measured on the road from Section II, to predict the maximum generated power. Since the harvester with the solid tip mass can be considered a linear system, the response is almost independent from input magnitude. Conversely, the response of the harvester with the liquid tip mass is dependent on the magnitude of the input (i.e.,

the base acceleration) [14]. For this reason, the tests involving the liquid tip mass were performed with the same acceleration RMS value measured on the road: 2.45 m/s^2 and 1.91 m/s^2 in the vertical and horizontal directions respectively.

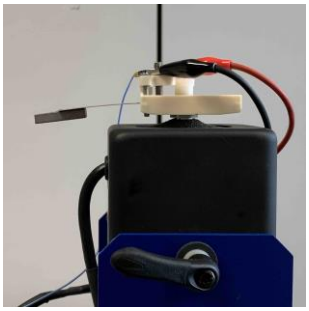

Fig. 11. Testing configuration for the harvester with solid tip mass, harvesting vertical vibrations.

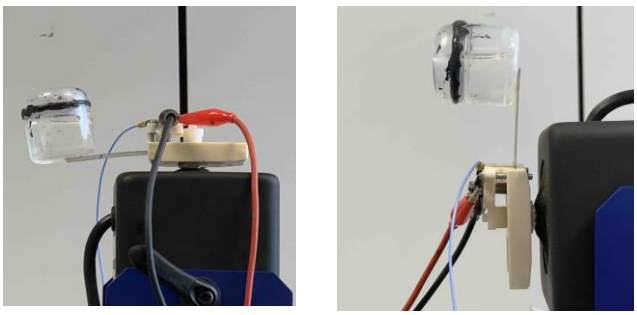

(a) (b)

Fig. 12. Testing configuration for the harvester with liquid tip mass, harvesting vertical (a) and horizontal (b) vibrations.

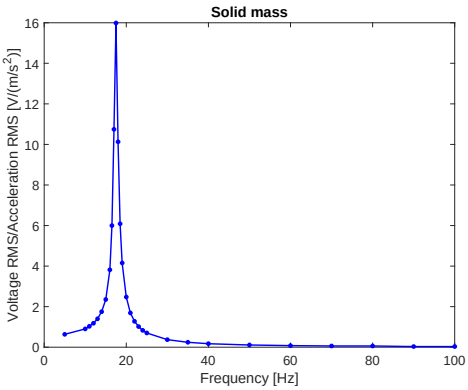

Fig. 13. Ratio between the RMS of generated voltage and the RMS of base acceleration, harvester with solid tip mass.

The results of the shaker tests are reported in Fig. 13 and Fig. 14, for the solid and liquid tip mass. Both types of tip mass are effective in lowering the natural frequency of the cantilever.

As for the tests in the vertical configuration, the solid tip mass causes a sharper, higher peak compared to the liquid tip mass, which in turn results in a wider bandwidth around the main resonance. Comparing the results obtained with the liquid tip mass in the two orientations, the main peak obtained with horizontal shaker axis has a higher frequency and a lower magnitude than the peak obtained with vertical shaker axis. This result is consistent with the analytical outcomes of Fig. 9 and Fig. 10, especially if large values of the damping ratios are used in the models.

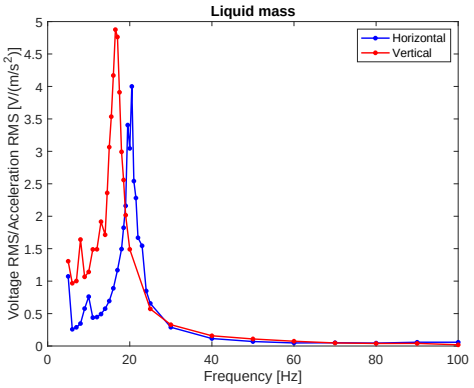

Fig. 14. Ratio between the RMS of generated voltage and the RMS of base acceleration, harvester with liquid tip mass.

VI. Prediction of Output Power

The PSD of the open-circuit voltage is estimated with (2) from the road-measured acceleration PSD (Section II) and the voltage-to-acceleration ratio is measured as discussed in Section V. The results of this calculation are shown in Fig. 15. The output voltage of the piezo-harvester is a random signal with a main harmonic component at the resonance vibration frequency of the cantilever. On the other hand, electronic devices are powered by DC input; therefore, a suitable power management unit (PMU) interfacing the harvester and the electronic load is required. A broadly used and appealing technique in the optimization of mechanical to electrical power conversion from vibrating structures is the synchronized switch harvesting on inductor (SSHI) technique [36]. By assuming harmonic excitation, the maximum average power generated by a SSHI rectifier can be estimated from the average RMS value of the open-circuit voltage V_{RMS}, with the procedure proposed in [15] and here briefly summarized. The maximum power extracted by the electronic converter is expressed as:

$$P_{max} = 2f\left(\frac{1+\gamma}{1-\gamma}\right)W_{max} \tag{19}$$

where f is the vibration frequency, γ is the inversion coefficient, and the maximum energy stored in the harvester is:

$$W_{max} = \frac{1}{2}\,C_{pu}V_{max}^2 \tag{20}$$

Due to the SSHI technique, the maximum charging voltage value is equal to the maximum open-circuit voltage, which under the harmonic excitation assumption is $V_{max} = \sqrt{2}\,V_{RMS}$. According to Parseval's theorem, an average RMS value is estimated from the open-circuit voltage PSD (2), as:

$$V_{RMS} = \sqrt{\int_0^{+\infty} S_{v0}(\omega)\,d\omega} \tag{21}$$

A capacitance value $C_{pu} = 0.1$ µF (taken from PPA-1001 datasheet [37]) and an inversion coefficient $\gamma = 0.76$ for the converter (typical value for SSHI-rectifier, as indicated in [18])

are assumed. Voltage and estimated power values for the harvester with liquid and solid tip masses, listed in Table I and Table II, are computed from PSDs in Fig. 15.

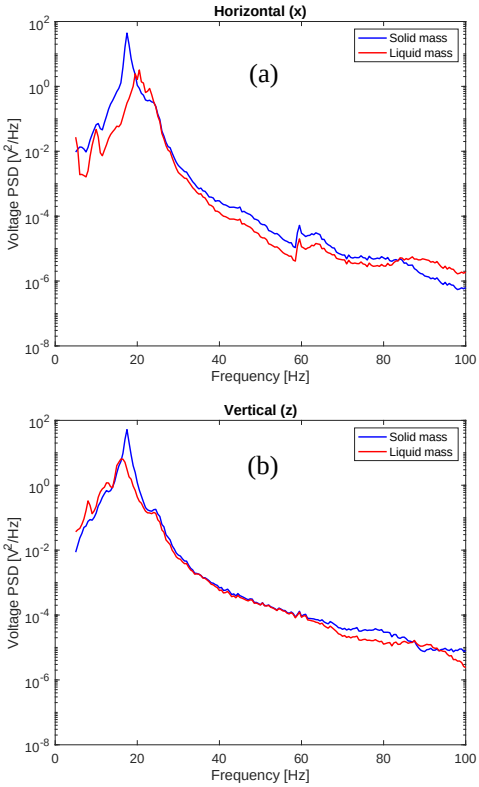

Fig. 15. Power spectral density of the generated voltage with solid and liquid tip masses: (a) horizontal direction, (b) vertical direction.

TABLE I
ESTIMATED RMS VOLTAGE (V) FOR HARVESTERS WITH SOLID AND LIQUID TIP MASSES

Direction	Solid tip mass	Liquid tip mass
Horizontal (x)	7.310	2.899
Vertical (z)	8.526	4.876

TABLE II
ESTIMATED ELECTRIC POWER (mW) FOR HARVESTERS WITH SOLID AND LIQUID TIP MASSES

Direction	Solid tip mass	Liquid tip mass
Horizontal (x)	1.372	0.253
Vertical (z)	1.866	0.558

As it would be expected from the experimentally-measured response discussed in Section V, the piezoelectric device equipped with the liquid tip mass is able to harvest less power compared to the solid tip mass. Nonetheless, the tuning with liquid may be preferable in some applications thanks to the lower mechanical stress and the consequently extended device lifetime. Moreover, it is worth noting that the harvester with no tuning device would exhibit much worse performance (P_{max}=0.2 μW) compared to tuned harvesters.

VII. PREDICTION OF STRESS

For a harvester with liquid tip mass the FRF between the maximum stress inside the piezo material and base acceleration $FRF_\sigma(\omega)$ can be calculated starting from the equation that gives the maximum bending stress at the clamped end:

$$S(t) = -h_c \left.\frac{\partial^2 w_r(x,t)}{\partial x^2}\right|_{x=0} \tag{22}$$

In which h_c in the maximum distance from the neutral axis of the composite cross section. Introducing (12) into (22) and considering the constitutive equation of a piezo material (3), this result is achieved:

$$FRF_\sigma(\omega) = -c_{11}^E\, h_c FRF_t(\omega) \left.\frac{\partial^2 g(x)}{\partial x^2}\right|_{x=0} + \frac{e_{31}}{h_{pu}} FRF_{\mathrm{OC}}(\omega) \tag{23}$$

$FRF_t(\omega)$ is the FRF between the harvester tip and base acceleration, h_{pu} the thickness of the piezo layer. Then the PSD of stress can be calculated as:

$$S_\sigma(\omega) = |FRF_\sigma(\omega)|^2\, S_A(\omega) \tag{24}$$

Numerical results obtained from (24) show a large stress reduction when the liquid mass is adopted (Fig. 16).

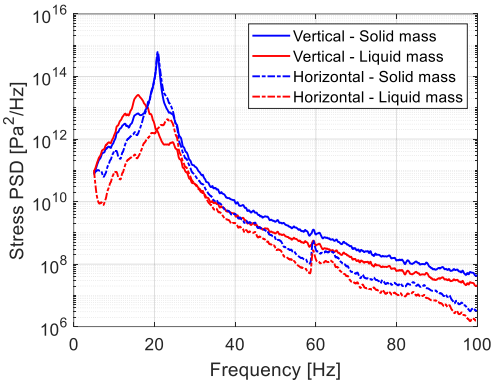

Fig. 16. Power spectral density of the generated stress with solid and liquid tip masses, maximum stress at the clamped end.

VIII. CONCLUSION

Numerical and experimental results show that a proper tuning is essential to improve the harvester's performance when mounted on a bike, which typically features low-frequency vibrations. Tuning devices based on liquid tip masses have been presented and tested. They are able to lower the resonance frequency of the harvester and to widen the bandwidth around resonance without excessively increasing the stress inside the piezo-layer. The proposed models can be useful for designing energy harvesting systems for powering on-board electronics in city bikes. Different tracks and mountain bikes will be considered in future developments of this work.

ACKNOWLEDGMENTS

The authors wish to acknowledge the partial financial support of University of Padova Project SID 2020 "Vibration energy harvesting from rain-drop impacts", PI Alberto Doria.

REFERENCES

[1] W. Lee, M. J. W. Schubert, B. Ooi, and S. J. Ho, "Multi-Source Energy Harvesting and Storage for Floating Wireless Sensor Network Nodes With Long Range Communication Capability," *IEEE Trans. on Industry Applications*, vol. 54, no. 3, pp. 2606-2615, May-June 2018, doi: 10.1109/TIA.2018.2799158.

[2] J. M. Lopera, H. del Arco Rodríguez, J. M. Pérez Pereira, A. R. de Castro, and J. L. Rendueles Vigil, "Practical Issues in the Design of Wireless Sensors Supplied by Energy Harvesting Thermoelectric Generators," *IEEE Trans. on Industry Applications*, vol. 55, no. 1, pp. 996-1005, Jan.-Feb. 2019, doi: 10.1109/TIA.2018.2867810.

[3] C. Wei and X. Jing, "A comprehensive review on vibration energy harvesting: Modelling and realization," *Renewable and Sustainable Energy Reviews*, vol. 74, pp. 1-18, 2017, doi: 10.1016/j.rser.2017.01.073.

[4] F. Pan, Z. Xu, L. Jin, P. Pan, and X. Gao, "Designed Simulation and Experiment of a Piezoelectric Energy Harvesting System Based on Vortex-Induced Vibration," *IEEE Trans. on Industry Applications*, vol. 53, no. 4, pp. 3890-3897, July-Aug. 2017, doi: 10.1109/TIA.2017.2687401.

[5] A. Doria, G. Fanti, G. Filipi, and F. Moro, "Development of a Novel Piezo-harvesterExcited by Raindrops," *Sensors*, vol. 19, no. 17, p. 3653, Aug. 2019, doi: 10.3390/s19173653.

[6] P. Chaudhary and P. Azad, "Energy Harvesting Using Shoe Embedded with Piezoelectric Material," *Journal of Elecronic Materials*, vol. 49, pp. 6455–6464, 2020, doi: 10.1007/s11664-020-08401-6.

[7] C. T. Pan, Y. J. Chen, Z. H. Liu, and C. H. Huang, "Design and fabrication of LTCC electro-magnetic energy harvester for low rotary speed", *Sensors and Actuators A: Physical*, vol. 191 pp. 51-60, 2013, doi: 10.1016/j.sna.2012.11.036

[8] Y. N. Chang, H. L. Cheng, S. Y. Chan, and L. H. Huang, "Electromagnetic Energy Harvester and Energy Storage System for Bike Lighting Applications," *Sensors and Materials*, vol. 30, no. 6, pp. 1341-1347, 2018, doi: 10.18494/SAM.2018.1782

[9] L. Buccolini and M. Conti, "An energy harvester interface for self-powered wireless speed sensor," *IEEE Sensors Journal*, vol. 17, no. 4, February 15, 2017, doi: 10.1109/JSEN.2016.2635940

[10] Y. Yang, J. Yeo, and S. Priya, "Harvesting energy from the counterbalancing (weaving) movement in bicycle riding", *Sensors*, vol. 12, pp. 10248-10258, 2012, doi: 10.3390/s120810248

[11] E. Minazara, D. Vasic, and F. Costa, "Piezoelectric generator harvesting bike vibrations energy to supply portable devices," *Renewable Energy and Power Quality Journal*, vol. 1, no. 6, pp. 508-513, March 2008, doi: 10.24084/repqj06.344.

[12] D. Vasic, Y. Y. Chen, and F. Costa, "Self-powered piezoelectric energy harvester for bicycle," *Journal of Mechanical Science and Technology*, vol. 28, no. 7, pp. 2501-2510, 2014, doi: 10.1007/s12206-014-0407-9.

[13] C. Jettanasen, P. Songsukthawan, and A. Ngaopitakkul, "Development of micro-mobility based on piezoelectric energy harvesting for smart city applications," *Sustainability*, vol. 12, no. 7, art. no. 2933, 2020, doi: 10.3390/su12072933.

[14] A. Doria, E. Marconi, and F. Moro, "Energy Harvesting From Bicycle Vibrations," in *Proc. of 2020 Fifteenth International Conference on Ecological Vehicles and Renewable Energies* (EVER), pp. 1-9, 2020, doi: 10.1109/EVER48776.2020.9243060.

[15] A. Doria, E. Marconi, and F. Moro, "Energy harvesting from bicycle vibrations by means of tuned piezoelectric generators," *Electronics*, vol. 9, art. no. 1377, 2020, doi:10.3390/electronics9091377.

[16] A. Doria, E. Marconi, L. Munoz, A. Polanco, and D. Suarez, "An experimental-numerical method for the prediction of on-road comfort of city bicycles," *Vehicle System Dynamics*, 2020, doi: 10.1080/00423114.2020.1759810.

[17] A. Doria, E. Marconi, and P. Cialoni, "Modal Analysis of a Utility Bicycle From the Perspective of Riding Comfort," in *Proc. ASME 2019 International Design Engineering Technical Conferences and Computers and Information in Engineering Conference (IDETC2019)*, Anaheim (CA), USA, August 18-21, 2019, doi: 10.1115/DETC2019-97277

[18] S. Priya and D. J. Inman, *Energy Harvesting Technologies*. New York (NY), USA: Springer, 2009. ISBN 978-0-387-76463-4.

[19] F. Okayasu, G. Ozeki, M. Mizuno, " Fatigue failure characteristics of lead zirconate titanate piezoelectric ceramics," *J. Eur. Ceram. Soc.*, vol. 30, pp. 713–725, 2010, doi: 10.1016/j.jeurceramsoc.2009.09.014.

[20] K. Kitagawa, T. Yamamoto, K. Kitagawa, "Cyclic fatigue behavior and mechanical properties of PZT piezoelectric ceramics, *J. Jpn. Soc. Powder Metallurgy*, vol. 52, no. 1, 2004, doi:10.2497/jjspm.52.16.

[21] M. Pole, B. Gamboa, A. Bhalla, R. Guo, "Degradation of piezoelectric device as an energy harvester under equivalent traffic stress condition", Ferroelectrics, vol. 540, no.1, 2019, doi: 10.1080/00150193.2019.1611110.

[22] N. Jackson, F. Stam, O. Z. Olszewski, H. Doyle, A. Quinn, and A. Mathewson, "Widening the bandwidth of vibration energy harvesters using a liquid-based non-uniform load distribution," *Sensors and Actuators A: Physical*, vol. 246, pp. 170-179, 2016.

[23] N. Jackson, F. Stam, O. Z. Olszewski, R. Houlihan, and A. Mathewson, "Broadening the Bandwidth of Piezoelectric Energy Harvesters Using Liquid Filled Mass," *Procedia Engineering*, vol. 120, pp. 328-332, 2015.

[24] X. Wu, J. Lin, S. Kato, K. Zhang, T. Ren, and L. Liu, "A Frequency Adjustable Vibration Energy Harvester", *Proc. of PowerMEMS*, Sendai, Japan, pp. 245-248, 2008.

[25] M. D. Dhone, P. G. Gawatre, and S. S. Balpande, "Frequency band widening technique for cantilever-based vibration energy harvesters through dynamics of fluid motion," *Materials Science for Energy Technologies*, vol. 1, no. 1, pp. 84-90, 2018, doi: 10.1016/j.mset.2018.06.002

[26] N. Jackson and F. Stam, "Sloshing liquid-metal mass for widening the bandwidth of a vibration energy harvester," *Sensors and Actuators A: Physical*, Vol. 284, pp. 17-21, 2018. doi:10.1016/j.sna.2018.10.010

[27] N. Jackson, "Tuning and widening the bandwidth of vibration energy harvesters using a ferrofluid embedded mass," *Microsystem Technologies*, Vol. 26, pp. 2043–2051, 2020. doi: 10.1007/s00542-020-04756-2

[28] R. Somkuwar, J.Chandwani, and R. Deshmukh, "Bandwidth widening of piezoelectric energy harvester by free moving cylinders in liquid medium," *Microsystem Technologies*, 2020. doi: 10.1007/s00542-020-04999-z

[29] R. A. Ibrahim, *Liquid Sloshing Dynamics, Theory and Applications*, Cambridge University Press, Cambridge UK, 2005.

[30] R. A. Ibrahim and V. N. Pilipchuk, "Recent advances in sloshing dynamics," *Appl Mech Rev*, Vol. 54, no. 2, March 2001.

[31] A. Kolaei, S. Rakheja, and M. J. Richard, "Range of applicability of the linear fluid sloshtheory for predicting transient lateral slosh and rollstability of tank vehicles," *Journal of Sound and Vibration*, Vol. 333, pp. 263–282, 2014.

[32] D. Liu, H. Li, H, Feng, T. Yalkun, and M. R. Hajj, "A multi-frequency piezoelectric vibrationenergy harvester with liquid filled containeras the proof mass," *Appl. Phys. Lett.* Vol. 114, 213902, 2019, doi: 10.1063/1.5089289.

[33] T. J. Kazmierski and S. Beeby, *Energy Harvesting Systems Principles, Modeling and Applications*, Springer, New York, 2011.

[34] A. Erturk and D.J. Inman, "An experimentally validated bimorph cantilever model for piezoelectric energy harvesting from base excitations," *Smart Mater. Struct.*, vol. 18, Art. no. 025009, 2009.

[35] K. A. Karamanos, L. A. Patkas, and M. A. Platyrrachos, "Sloshing Effects on the Seismic Design of Horizontal-Cylindrical and Spherical Industrial Vessels", *ASME J. Pressure Vessel Technol.* Aug 2006, Vol. 128(3), pp. 328-340, doi.org/10.1115/1.2217965.

[36] J. Dicken, P. D. Mitcheson, I. Stoianov, and E. M. Yeatman, "Power-Extraction Circuits for Piezoelectric Energy Harvesters in Miniature and Low-Power Applications," *IEEE Transactions on Power Electronics*, vol. 27, no. 11, pp. 4514–4529, 2012, doi: 10.1109/TPEL.2012.2192291.

[37] *User Manual, Piezo protection advantage*, Midè, Rev. No. 001, 1-12-2016. Accessed on: July, 30, 2021. [Online]. Available: https://cdn2.hubspot.net/hubfs/3841176/Data-Sheets/ppa-piezo-product-datasheet.pdf

Alberto Doria received the Laurea degree (honors) in Mechanical Engineering (University of Padova 1984). Then he joined the Italian Research Authority, becoming member of the design group of RFX, an Euratom fusion experiment. He received the Specialization in Plasma Engineering and Controlled Thermonuclear Fusion (University of Padova 1987).
Alberto Doria in 1990 joined the University of Padova. Now Alberto Doria is full professor of Machine Mechanics of the University of Padova, he coordinates the activities on Mechanical Vibrations in the laboratories of Modal Analysis and Vibration Mechanics. The present research topics are mechanics, vibrations, identification, robot vibrations, vibration energy harvesting.

Edoardo Marconi is a Ph.D. in Mechanical Engineering. He received a Bachelor's degree (with honors) in Mechanical Engineering in 2013, a Master's degree (with honors) in Mechanical Engineering in 2016, and a Ph.D. in Mechanical Engineering in 2021, all from the University of Padova.
In 2016-2017 he was a research fellow at the Department of Industrial Engineering of the University of Padova, studying the numerical simulation of wearable airbags for motorcyclists, in collaboration with Dainese SpA. His Ph.D. research (2017-2020) dealt with different topics in vehicle dynamics, such as minimum-lap-time optimal control simulation of racing motorcycles, ride comfort, and two-wheeled vehicle stability. Currently, he is a postdoctoral research fellow at the Department of Industrial Engineering of the University of Padova, researching vibration energy harvesting from rain-drop impacts.
His research interests include vehicle dynamics and control, modal analysis, multibody simulation, vibration energy harvesting.

Federico Moro (Member IEEE) Federico Moro received the Laurea degree in Electrical Engineering (2003), the Ph.D. degree in Bioelectromagnetic and Electromagnetic Compatibility (2007), and the B.S. degree in Mathematics (2012) from the University of Padova, Italy. He obtained the National Scientific Qualification as Full Professor (09/E1-Elettrotecnica) in 2021. From 2007 to 2010 he was a Research Associate at the Department of Electrical Engineering, University of Padova. From 2010 to 2020 he was an Assistant Professor of Electrical Engineering at the Department of Industrial Engineering of the same university. Since 2020 he is an Associate Professor of Electrical Engineering at the same department.
His research interests include numerical methods for computing electromagnetic problems and the numerical modeling of multiphysics and multiscale problems. He is author of more than 100 articles in peer-reviewed international journals and conference proceedings.